

University of Groningen

## Electron heating by photon-assisted tunneling in niobium terahertz mixers with integrated niobium titanium nitride striplines

Leone, B.; Gao, J. R.; Klapwijk, T. M.; Jackson, B. D.; Laauwen, W. M.; de Lange, G.

*Published in:*  
Applied Physics Letters

*DOI:*  
[10.1063/1.1355003](https://doi.org/10.1063/1.1355003)

**IMPORTANT NOTE: You are advised to consult the publisher's version (publisher's PDF) if you wish to cite from it. Please check the document version below.**

*Document Version*  
Publisher's PDF, also known as Version of record

*Publication date:*  
2001

[Link to publication in University of Groningen/UMCG research database](#)

*Citation for published version (APA):*

Leone, B., Gao, J. R., Klapwijk, T. M., Jackson, B. D., Laauwen, W. M., & de Lange, G. (2001). Electron heating by photon-assisted tunneling in niobium terahertz mixers with integrated niobium titanium nitride striplines. *Applied Physics Letters*, 78(11), 1616-1618. <https://doi.org/10.1063/1.1355003>

### Copyright

Other than for strictly personal use, it is not permitted to download or to forward/distribute the text or part of it without the consent of the author(s) and/or copyright holder(s), unless the work is under an open content license (like Creative Commons).

The publication may also be distributed here under the terms of Article 25fa of the Dutch Copyright Act, indicated by the "Taverne" license. More information can be found on the University of Groningen website: <https://www.rug.nl/library/open-access/self-archiving-pure/taverne-amendment>.

### Take-down policy

If you believe that this document breaches copyright please contact us providing details, and we will remove access to the work immediately and investigate your claim.

Downloaded from the University of Groningen/UMCG research database (Pure): <http://www.rug.nl/research/portal>. For technical reasons the number of authors shown on this cover page is limited to 10 maximum.

# Electron heating by photon-assisted tunneling in niobium terahertz mixers with integrated niobium titanium nitride striplines

B. Leone, J. R. Gao, T. M. Klapwijk, B. D. Jackson, W. M. Laauwen, and G. de Lange

Citation: *Appl. Phys. Lett.* **78**, 1616 (2001); doi: 10.1063/1.1355003

View online: <https://doi.org/10.1063/1.1355003>

View Table of Contents: <http://aip.scitation.org/toc/apl/78/11>

Published by the [American Institute of Physics](#)

---

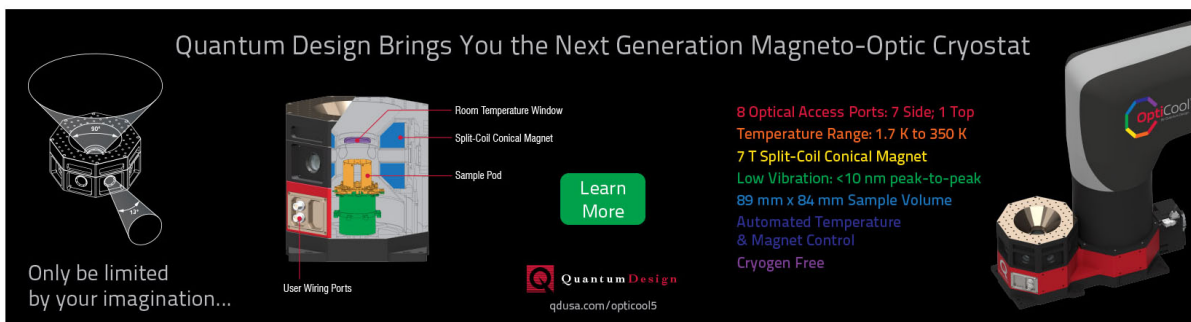
## Articles you may be interested in

[Hot-electron bolometer terahertz mixers for the Herschel Space Observatory](#)

*Review of Scientific Instruments* **79**, 034501 (2008); 10.1063/1.2890099

---

Quantum Design Brings You the Next Generation Magneto-Optic Cryostat



Only be limited by your imagination...

Room Temperature Window  
Split-Coil Conical Magnet  
Sample Pod  
User Wiring Ports

[Learn More](#)

Quantum Design  
qdusa.com/opticool5

8 Optical Access Ports: 7 Side; 1 Top  
Temperature Range: 1.7 K to 350 K  
7 T Split-Coil Conical Magnet  
Low Vibration: <10 nm peak-to-peak  
89 mm x 84 mm Sample Volume  
Automated Temperature & Magnet Control  
Cryogen Free

# Electron heating by photon-assisted tunneling in niobium terahertz mixers with integrated niobium titanium nitride striplines

B. Leone

Material Science Center, University of Groningen, 9747 AG Groningen, The Netherlands

J. R. Gao<sup>a)</sup> and T. M. Klapwijk

Department of Applied Physics and DIMES, Delft University of Technology, 2628 CJ Delft, The Netherlands

B. D. Jackson, W. M. Laauwen, and G. de Lange

Space Research Organization Netherlands, P.O. Box 800, 9700 AV Groningen, The Netherlands

(Received 13 July 2000; accepted for publication 10 January 2001)

We describe the gap voltage depression and current–voltage ( $I$ – $V$ ) characteristics in pumped niobium superconductor–insulator–superconductor junction with niobium titanium nitride tuning stripline by introducing an electron heating power contribution resulting from the photon-assisted tunneling process. Theoretical fits using the extended Tien–Gordon theory are obtained that reproduce the most salient features of the pumped  $I$ – $V$  characteristics. © 2001 American Institute of Physics. [DOI: 10.1063/1.1355003]

The lowest noise temperature around 1 THz has been obtained using a Nb superconductor–insulator–superconductor (SIS) mixer with a hybrid tuning stripline consisting of a NbTiN bottom layer and an Al top layer sandwiching the SiO<sub>2</sub> dielectric.<sup>1</sup> The use of this hybrid stripline leads to a dramatic improvement of the mixer sensitivity as compared with the all aluminum stripline results.<sup>2</sup> This is to be expected since a major limiting factor of the mixer performance is the loss in the aluminum<sup>3</sup> and, conversely, superconducting NbTiN has been shown to be a good candidate material to minimize low rf losses.<sup>4</sup> On the basis of these promising results alone, one can hope for a further sensitivity improvement with an all NbTiN stripline. At the same time, the presence of an energy gap discontinuity between Nb and NbTiN is expected to give rise to undesirable effects which might degrade mixer performance. Both dc and rf heating on the current–voltage ( $I$ – $V$ ) characteristics was observed experimentally in such devices.<sup>5</sup> In particular, rf heating can severely reduce the gap and affect the pumped  $I$ – $V$  characteristics. The dc heating effect was analyzed and understood.<sup>6</sup> In this letter, we will focus on the analysis of the rf heating effect, which we believe to be more important to the field of SIS mixers than the dc heating for two reasons. Technologically, the pumped  $I$ – $V$  curves are more relevant to the mixer performance. Fundamentally, the heating effect due to different rf pumping is an unexplored subject in SIS mixers.

Our device consists of a Nb junction sandwiched between two NbTiN leads, which, in combination with an insulator SiO<sub>2</sub> layer, form a stripline that functions as an integrated tuning circuit for the mixer. The junction is a standard Nb/Al–AlO<sub>x</sub>/Nb structure with an area of typically 0.6 μm<sup>2</sup> and a critical current density of 12 kA/cm<sup>2</sup>. The device geometry is the same as in Ref. 6. The  $I$ – $V$  measurements at

various pumping level achieved through a local oscillator (LO) operating near 1 THz and via a wave guide have been reported previously<sup>5</sup> and are partly reproduced in Fig. 1. The most striking feature is the severe gap depression increasing with pumping level, i.e., from the unpumped curve A to curve D, which has nearly undergone the transition to the normal state. Another feature corresponds to the gap depression taking place within a curve called backbending because the resulting  $I$ – $V$  curve bends backwards. Backbending was quantitatively analyzed in the unpumped case as being caused by the presence of the gap discontinuity at the Nb/NbTiN interface.<sup>6</sup> The results can be summarized as follows. The energy diagram in the inset of Fig. 1 shows the different energy gaps of Nb and NbTiN and a quasiparticle tunneling through the junction barrier when the two electrodes are biased at the Nb gap voltage. The electrons see a potential barrier at the Nb/NbTiN interface. As a result, there is no

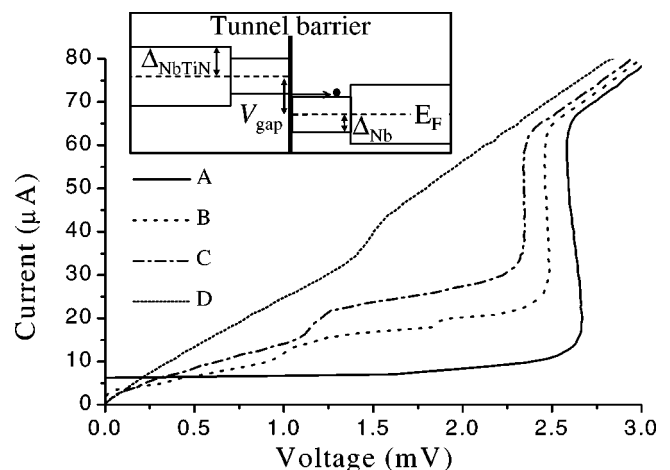


FIG. 1.  $I$ – $V$  characteristics of a Nb/Al–AlO<sub>x</sub>/Nb junction with NbTiN striplines at a local oscillator frequency of 895 GHz and a bath temperature of 4.7 K for increasing pumping level from A (unpumped) to D. Inset: Energy diagram showing the relative energy gaps of Nb and NbTiN under the application of a bias voltage  $V_{\text{gap}}$  equal to the gap voltage of Nb.

<sup>a)</sup>Also with Space Research Organization Netherlands, Utrecht, The Netherlands; electronic mail: j.r.gao@tnw.tudelft.nl

diffusion cooling. However, Andreev reflection of the electrons into NbTiN prevents charge accumulation at the interface. By assuming a Fermi-like electron energy distribution, this leads to an increased junction electron temperature  $T$  which is obtained from the gap voltage data using the Bardeen–Cooper–Schrieffer theory of superconductivity.<sup>7</sup> Finally, knowledge of the dc input power and the heat flow bottleneck leads to the following heat balance equation:

$$P_{dc} = \alpha(T - T_b), \quad (1)$$

where  $T_b$  is the bath temperature and  $\alpha$  the heat transfer coefficient. Equation (1) is approximately valid for small temperature differences as shown in Ref. 6, where agreement with the dc  $I$ – $V$  characteristics was demonstrated, leading to the coefficient  $\alpha$  to be  $1.3 \times 10^{-7}$  W/K. Analysis of rf heating using the heat balance equation with  $T^4$  dependence has also been performed,<sup>8</sup> giving no essential difference in the outcome.

As the rf signal is coupled into the mixer,  $P_{dc}$  is no longer the total available input power so that the severe gap reduction shown in Fig. 1 cannot be explained by  $P_{dc}$  only. Essentially, there are two additional power sources in the pumped case. The first one is the photon-assisted tunneling (PAT) mechanism which is responsible for the energy spectrum of the photon-assisted tunneled electrons according to the Tien–Gordon picture.<sup>9</sup> The second is the rf absorption in the junction that comes about through the breaking of Cooper pairs above the gap frequency of Nb. In standard junctions both contributions escape by thermal conduction. However, in the presence of heat trapping they will have to be dissipated within the electron bath, thus contributing to the overall junction heating. As will become clear, the rf absorption contribution is negligible so we turn our attention to the PAT mechanism. Each photon-assisted electron has an energy that depends on its energy before tunneling and the number of photons absorbed during the tunneling process. The Tien–Gordon theory<sup>9</sup> pictures that the tunneling current corresponding to  $n$  photons of energy  $\hbar\omega$  absorbed per tunneling process is given by the measured unpumped characteristic  $I_{dc}$ , shifted by  $n\hbar\omega/e$ , and weighed by the corresponding  $n$ th order Bessel function of the first kind  $J_n$ . The total pumped  $I$ – $V$  characteristic  $I_{rf}$ , as a function of the bias voltage  $V$  is obtained by summing all contributions, i.e.,

$$I_{rf}(V) = \sum_{n=-\infty}^{\infty} J_n^2(eV_{LO}/\hbar\omega) I_{dc}(V + n\hbar\omega/e). \quad (2)$$

The Bessel function factor arises from the inclusion of a sinusoidal rf field in the Schrödinger equation for the quasiparticle wave function. Its argument contains  $V_{LO}$ , the voltage across the junction associated to the LO power.  $I_{rf}$  is characterized by regions of enhanced current below the gap, and diminished current above it, called photon steps. Using the Tucker–Feldman theory<sup>10</sup> one can infer the embedding impedance of the mixer, and thereby the bias voltage dependence of  $V_{LO}$  from the slope of the photon step. However, for simplicity, we follow Tien and Gordon<sup>9</sup> in assuming a constant  $V_{LO}$  over the entire bias voltage range. This is then used to fit photon step levels through Eq. (2). The corre-

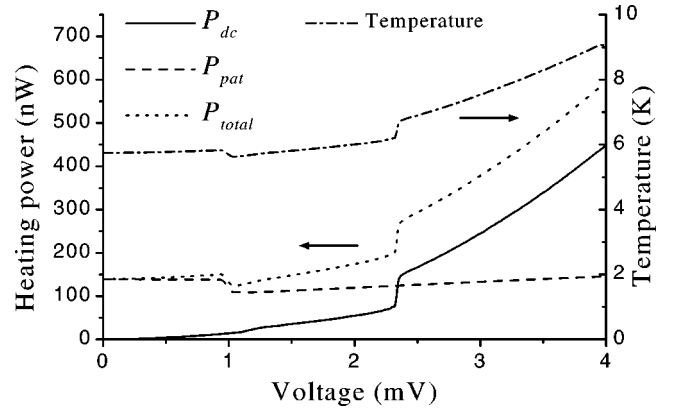


FIG. 2. The heating powers corresponding to the dc, PAT, and total contributions as a function of bias voltage, calculated for curve C in Fig. 1, are shown together with the junction temperature inferred from the total power.

sponding heating power,  $P_{pat}$ , is obtained by multiplying each current contribution in Eq. (2) by its corresponding photon energy multiple in voltage units, i.e.,

$$P_{pat} = \sum_{n=-\infty}^{\infty} \frac{n\hbar\omega}{e} J_n^2(eV_{LO}/\hbar\omega) I_{dc}(V + n\hbar\omega/e). \quad (3)$$

We note that Eqs. (2) and (3) are both  $V_{LO}$ -dependent. The significance of this will become clearer in the following example. Let us choose curve C in Fig. 1, which corresponds to a pumping level not unlike what is used in actual detection, and calculate the power contributions to the heat trapping mechanism.  $P_{dc}$  is given by the product of the current by the voltage at each bias point of curve C. The photon-assisted power  $P_{pat}$ , is calculated using Eq. (3) for  $V_{LO} = 3.18$  mV and where  $I_{dc}(V)$  is taken to be the unpumped measured data, i.e., curve A in Fig. 1. The value chosen for  $V_{LO}$  will become clear below.  $P_{dc}$ ,  $P_{pat}$ , and their sum  $P_{total}$  as a function of bias voltage are plotted in Fig. 2. It should be noted here that, whereas  $P_{dc}$  increases with bias voltage,  $P_{pat}$  is already substantial at zero bias voltage and does not change appreciably thereafter except for a glitch around 1 mV. This point corresponds to the negative gap of  $I_{dc}$  shifted by  $\hbar\omega/e$ , i.e., it results from the addition of the  $n = 1$  and  $n = -1$  contributions of Eq. (3). Now, by replacing  $P_{dc}$  in Eq. (1) with the total power contribution  $P_{total}$  one obtains the effective electron temperature in the Nb junction in the pumped case as a function of bias voltage  $T(V)$ . This is also shown in Fig. 2. The corresponding unpumped theoretical  $I$ – $V$  characteristic can be calculated using the Fermi Golden Rule twice

$$I_{cal} = \frac{1}{eR_n} \int_{-\infty}^{\infty} N(E)N(E - eV)[f(E - eV) - f(E)]dE, \quad (4)$$

where  $R_n$  is the normal state resistance. Here care is taken that the Fermi–Dirac distribution function  $f(E)$  and the density of states  $N(E)$  be made explicit functions of the bias voltage-dependent electron temperature  $T(V)$

$$N(E) = \frac{E}{\sqrt{E^2 - \Delta^2(T(V))}}, \quad (5)$$

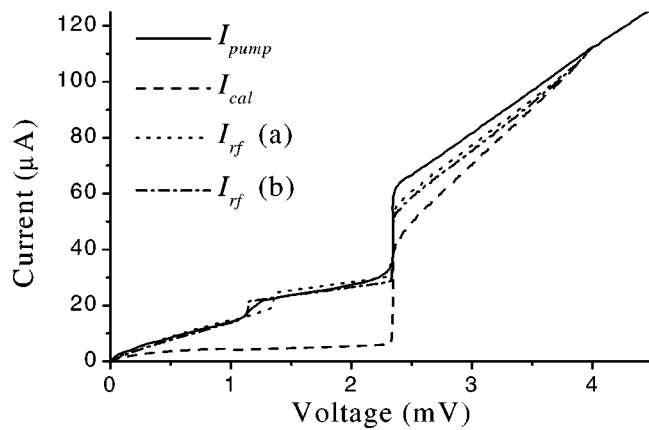


FIG. 3.  $I_{\text{pump}}$  represents the measured pumped  $I$ - $V$  curve and corresponds to curve C in Fig. 1;  $I_{\text{cal}}$  is the theoretical unpumped curve calculated using the bias voltage-dependent temperature  $T(V)$ , shown in Fig. 2; the two  $I_{\text{rf}}$  curves are obtained by (a) inserting  $I_{\text{cal}}$  into Eq. (2), and (b) by calculating  $I_{\text{cal}}$  directly within Eq. (2).

$$f(E) = \frac{1}{\exp(E/kT(V)) + 1}. \quad (6)$$

Figure 3 shows  $I_{\text{cal}}$  calculated using  $T(V)$ . Worthy of note is that  $I_{\text{cal}}$  has the same gap voltage as the pumped data. However, this results from our choice of  $V_{\text{LO}}$ . One should check this choice by replacing  $I_{\text{dc}}$  with  $I_{\text{cal}}$  into Eq. (2). This yields the calculated pumped  $I$ - $V$  characteristic  $I_{\text{rf}}$ , shown in Fig. 3 as  $I_{\text{rf}}$  (a), which fits both the depressed gap and the photon step level using a single fitting parameter  $V_{\text{LO}}$ . Our physical picture is thereby self-consistent. Nevertheless, the calculated  $I$ - $V$  characteristic fails to reproduce the correct photon step onset. In fact, Eq. (2) implicitly assumes the photon step onset and the gap voltage to occur at the same temperature. Dependence on  $T(V)$  is ensured, however, by using Eq. (4) to calculate each current contribution shifted by  $n\hbar\omega/e$  separately before carrying out the summation in Eq. (2). The resulting fit  $I_{\text{rf}}$  (b) in Fig. 3, agrees well with the experimental photon step onset.

Similar fits were obtained for different local oscillator frequencies, pumping levels, bath temperatures, and current density devices with  $V_{\text{LO}}$  being the only fitting parameter. The fitting procedure is therefore robust. By close inspection of Fig. 3 it can be seen that, in addition to the gap depression, the photon step level and the photon step onset already mentioned, the fitted subgap current also agrees well with experiment. There are also deviations from the data. First,

the smoothing in the measured photon step and gap which can be ascribed to quasiparticle lifetime effects.<sup>11</sup> Second, since we considered a constant  $V_{\text{LO}}$  the fitted curves are generally flatter than in the experimental data. Third, the excess current in the measured data just above the gap can be explained by the deviation from the ideal SIS structure of the actual junctions, which more closely resemble a superconductor-normal metal-insulator-superconductor structure.<sup>12</sup>

In conclusion, we recognize very different heat trapping behaviors for the PAT cases. The heat power due to PAT is quite substantial in the subgap regime and is present even at zero bias voltage in contrast with the dc heating. By introducing the bias-voltage dependent electron heating, taking both PAT and dc heating into account, in the Tien-Gordon theory, we are able to reproduce the measured pumped  $I$ - $V$  curves. Finally, an offshoot of our analysis is that the rf absorption contribution in the Nb junction should be negligibly small since PAT is more than sufficient to explain the pumped data.

One of the authors (B.L.) gratefully acknowledges B.J. van Wees for his support and helpful discussion. This work was partly supported by the European TMR network for Terahertz electronics (INTERACT).

- <sup>1</sup>B. D. Jackson, A. M. Baryshev, G. de Lange, J. R. Gao, S. V. Shitov, N. N. Iosad, and T. M. Klapwijk, Appl. Phys. Lett. (submitted).
- <sup>2</sup>M. Bin, M. C. Gaidis, J. Zmuidzinas, T. G. Phillips, and H. G. LeDuc, Appl. Phys. Lett. **68**, 1714 (1996).
- <sup>3</sup>P. Dieleman, T. M. Klapwijk, J. R. Gao, and H. van de Stadt, IEEE Trans. Appl. Supercond. **7**, 2566 (1997).
- <sup>4</sup>J. Kawamura, J. Chen, D. Miller, J. W. Kooi, J. Zmuidzinas, B. Bumble, H. G. LeDuc, and J. H. Stern, Appl. Phys. Lett. **75**, 4013 (1999), and references therein.
- <sup>5</sup>B. D. Jackson, N. N. Iosad, B. Leone, J. R. Gao, T. M. Klapwijk, W. M. Laauwen, G. de Lange, and H. van de Stadt, Proceedings of the Xth International Symposium on Space Terahertz Technology, University of Virginia, March 1999, pp. 144-156.
- <sup>6</sup>B. Leone, B. D. Jackson, J. R. Gao, and T. M. Klapwijk, Appl. Phys. Lett. **76**, 780 (2000).
- <sup>7</sup>M. Tinkham, *Introduction to Superconductivity*, 2nd ed. (McGraw-Hill, New York, 1996), p. 63.
- <sup>8</sup>B. Leone, J. R. Gao, T. M. Klapwijk, B. D. Jackson, W. M. Laauwen, and G. de Lange, IEEE Trans. Appl. Supercond. (in press).
- <sup>9</sup>P. K. Tien and J. P. Gordon, Phys. Rev. **129**, 647 (1963).
- <sup>10</sup>J. R. Tucker and M. J. Feldman, Rev. Mod. Phys. **57**, 1055 (1985).
- <sup>11</sup>L. Solymar, *Superconductive Tunneling and Applications* (Chapman and Hall, London, 1972), p. 43.
- <sup>12</sup>E. L. Wolf, *Principles of Electron Tunneling Spectroscopy* (Oxford University Press, New York, 1985), p. 184.